Acta Crystallographica Section C
**Crystal Structure
Communications**
ISSN 0108-2701

Lithium vanadate $Li_{3+x}V_6O_{13}$ at low temperature

Jonas Höwing, Torbjörn Gustafsson* and John O. Thomas

Department of Materials Chemistry, Ångström Laboratory, Uppsala University,
Box 538, SE-751 21 Uppsala, Sweden
Correspondence e-mail: tgn@mkem.uu.se

Received 5 February 2004
Accepted 21 May 2004
Online 22 June 2004

The structure of $Li_{3+x}V_6O_{13}$ [x = 0.24 (3)] at 95 K has been solved and refined using single-crystal X-ray diffraction. The refined lithium content corresponds to two fully occupied Li sites and one partially occupied Li site. A doubling of the *c* axis is observed upon cooling from room temperature, and this change is associated with shifts of the V atoms. The resulting space group is *C*2/*c*. The Li disorder present in the $Li_3V_6O_{13}$ phase at room temperature is also observed in the low-temperature phase reported here.

Comment

Over the past two decades, V_6O_{13} has been investigated thoroughly as a possible cathode material for lithium polymer batteries. The V_6O_{13} structure was first solved by von Aebi (1948) and was later refined by Wilhelmi *et al.* (1971). The crystal system is monoclinic, in space group *C*2/*m*, and the structure is built of edge- and corner-sharing VO_6 octahedra, forming alternating single and double layers. Large channels occur between these layers, along the *b* direction, thus allowing Li^+ ions to diffuse easily through the V_6O_{13} host. Several stoichiometric phases are formed during lithium insertion, with $Li_6V_6O_{13}$ as the end phase. So far, the structure of $Li_xV_6O_{13}$ has been determined for $x = \frac{2}{3}$, 1, 2 and 3 (Björk *et al.*, 2001; Bergström *et al.*, 1997, 1998). The formation of superstructures was observed in $Li_{2/3}V_6O_{13}$ and LiV_6O_{13}, with tripling and doubling of the unit-cell volume, respectively. The original V_6O_{13} unit cell is again observed for $Li_2V_6O_{13}$ and $Li_3V_6O_{13}$, with only small changes in cell parameters. In all $Li_xV_6O_{13}$ structures determined so far, including those with superstructures, all atoms are situated in the mirror planes of the *C*2/*m* space group. In $Li_3V_6O_{13}$, one of the Li^+ ions is disordered across an inversion centre in the *ab* plane, *i.e.* in the single layer of the V_6O_{13} host structure. This disordered Li^+ ion was refined as two partially occupied sites, above and below the inversion centre, and showed relatively large displacement parameters.

V_6O_{13} has been reported to undergo a semiconductor–semiconductor phase transition at *ca* 150 K (Kachi *et al.*, 1963). The low-temperature structure of V_6O_{13} has been reinvestigated recently, and the phase-transition temperature was determined to be 153 K (Höwing *et al.*, 2003). That study showed that, on passing through the phase transition, all atoms move out of the mirror plane, thus destroying the C-centring and replacing the mirror plane by a glide plane; the new space group is *Pc*. The largest displacements [0.21 (1) Å] occur for the V atoms in the single octahedral layer, with possible partially occupied sites on opposite sides of the glide plane. Unfortunately, this disorder was not characterized further.

In the present study, $Li_{3+x}V_6O_{13}$ [x = 0.24 (3)] has been investigated at 95 K using single-crystal X-ray diffraction. It is found that a superlattice is formed, with a doubling of the *c* axis compared with that of the room-temperature structure (Höwing *et al.*, 2004). The mirror plane in *C*2/*m* is replaced by a glide plane, and an I-centred supercell is formed with the space group *I*2/*a*. The standard space-group setting, *C*2/*c*, is achieved through cell-axis transformation. The refined structure, with *C*2/*c* symmetry, is shown in Fig. 1, and selected interatomic distances are given in Table 1. The 2*c* double unit cell is closely related to the supercell of LiV_6O_{13}, although the reason for the supercell formation is quite different. In LiV_6O_{13}, the superlattice is formed by long-range interactions between lithium ions inserted into adjacent unit cells. In the

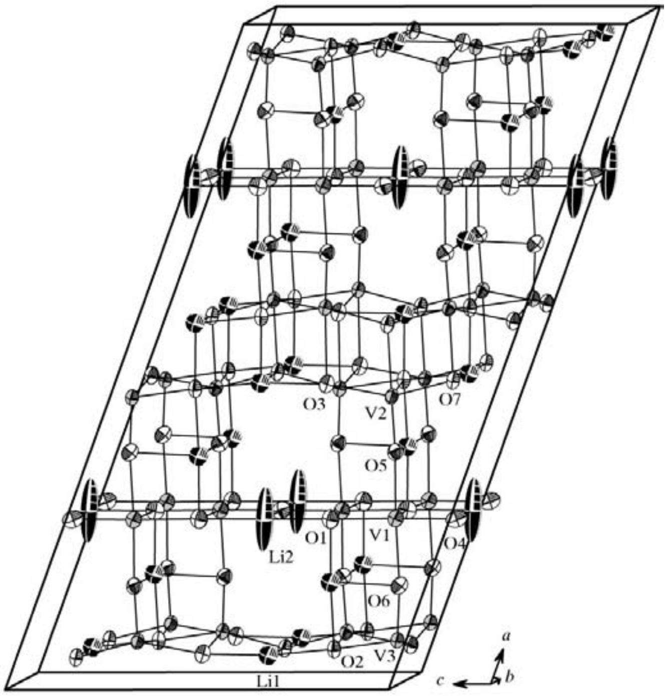

Figure 1
The low-temperature structure of $Li_{3.24}V_6O_{13}$. For clarity, the cell has been extended in the *b* direction to incorporate 1.5 unit cells. Displacement ellipsoids and spheres are drawn at the 90% probability level. O, V and Li atoms are shown in white, grey and black, respectively. The Li2 displacement ellipsoid describes two equivalent sites, above and below the inversion centre, and their partial overlap.

DOI: 10.1107/S0108270104012508

present structure, the double *c* axis results from the movement of atoms V2 and V3 away from or towards one another in alternate double octahedral layers. The phase composition, $Li_{3.24}V_6O_{13}$, was derived by refining the occupancy of the Li3 site and is in reasonable agreement with that expected from the sample preparation (see *Experimental*). In contrast to V_6O_{13}, where the largest atom shifts occur in the single layer, it is the V atoms in the double layer that undergo the largest displacements in the title compound, although the maximum displacement is only 0.04 (1) Å for atom V2, and the shifts are less than 3σ for most atoms. The differences in bond lengths between the room- and low-temperature structures are very small. Only the V2—O and V3—O distances along the *b* direction show any significant changes. As the V atoms move out of the original mirror planes, one V—O bond becomes longer while the opposite bond becomes correspondingly shorter.

Another interesting feature is that there is no observable change in the Li2 ion distribution in the single layer at low temperature. If this disorder were dynamic at room temperature on a time scale shorter than that of the diffraction process, it is likely that some ordering would occur upon cooling. Since this is not the case, it is concluded that the Li2 atom is not oscillating between two equivalent sites but, rather, is statically disordered. The movement of atom Li2 out of the square-planar oxygen coordination environment is thought to be a result of the long distance to any neighbouring atoms above or below the square. This hypothesis is consistent with observations for $Li_xV_6O_{13}$ ($x = \frac{2}{3}$, 1 and 2), where the Li atom is positioned slightly outside a square-planar–pyramidal oxygen coordination environment. The phase-transition temperature has not been determined more precisely.

Experimental

The diffraction experiment was carried out on beamline I711 at MAX-lab in Lund, Sweden (Cerenius *et al.*, 2000). Single crystals of V_6O_{13} were grown using the chemical vapour transport (CVT) technique described by Saeki *et al.* (1973). V_6O_{13} powder was synthesized using controlled thermal decomposition of NH_4VO_3, as described by Lampe-Önnerud & Thomas (1995). Powder cathodes were prepared by ball-milling together the as-synthesized V_6O_{13} powder, carbon black and EPDM (ethylene propylene diene copolymer) dissolved in cyclohexene, in a 80:15:5 mass% ratio. The cathode slurry was spread onto aluminium foil using a wire bar and 2.0 cm-diameter cathodes were punched out. Five V_6O_{13} single crystals were then incorporated into the powder cathode and the cathode was incorporated into a test-cell of 'coffee-bag' type (Gustafsson *et al.*, 1992). The electrolyte was 1 *M* $LiPF_6$ in EC/DMC (ethylene carbonate/dimethyl carbonate) in a 2:1 *v*/*v* mixture. The cell was discharged potentiostatically to 2.45 V, corresponding to the approximate composition $Li_3V_6O_{13}$. The battery was then held at this potential to equilibrate for two months, and was subsequently discharged further to 2.30 V (approximate composition for $Li_{3.4}V_6O_{13}$) and left to equilibrate for one more month. The cell was finally disassembled and the crystals were recovered. All crystals shattered during this electrochemical lithiation process. One piece with the approximate dimensions 0.05 × 0.02 × 0.01 mm was attached to a glass fibre for single-crystal data collection.

Table 1
Selected interatomic distances (Å).

$V1—O1^{i}$	1.964 (4)	$V3—O7^{v}$	1.956 (1)
$V1—O1^{ii}$	1.968 (4)	$Li1—O2$	2.024 (6)
$V1—O4$	1.8598 (5)	$Li1—O2^{vi}$	1.979 (6)
$V1—O5$	1.986 (2)	$Li1—O3^{vii}$	2.011 (5)
$V1—O6$	2.012 (2)	$Li1—O7^{i}$	1.974 (9)
$V2—O2^{i}$	1.999 (4)	$Li1—O7^{ii}$	1.948 (9)
$V2—O2^{ii}$	1.959 (4)	$Li2—O1$	2.012 (3)
$V2—O3$	2.001 (1)	$Li2—O1^{vii}$	2.012 (3)
$V2—O5$	1.661 (2)	$Li2—O4^{i}$	1.960 (1)
$V2—O7$	1.961 (2)	$Li2—O4^{ii}$	1.960 (1)
$V2—O7^{iii}$	2.169 (2)	$Li3—O1$	1.89 (4)
$V3—O2$	1.974 (2)	$Li3—O2$	2.01 (4)
$V3—O3^{i}$	1.988 (4)	$Li3—O5^{i}$	2.00 (8)
$V3—O3^{ii}$	2.021 (4)	$Li3—O5^{ii}$	1.94 (8)
$V3—O3^{iv}$	2.294 (2)	$Li3—O6$	2.12 (4)
$V3—O6$	1.642 (2)		

Symmetry codes: (i) $\frac{1}{2}-x, y-\frac{1}{2}, \frac{1}{2}-z$; (ii) $\frac{1}{2}-x, \frac{1}{2}+y, \frac{1}{2}-z$; (iii) $1-x, y, \frac{1}{2}-z$; (iv) $x-\frac{1}{2}, \frac{1}{2}-y, z-\frac{1}{2}$; (v) $\frac{1}{2}-x, \frac{1}{2}-y, -z$; (vi) $-x, y, \frac{1}{2}-z$; (vii) $\frac{1}{2}-x, \frac{1}{2}-y, 1-z$.

Crystal data

$Li_{3.24}V_6O_{13}$
$M_r = 536.3$
Monoclinic, $C2/c$
$a = 21.487$ (5) Å
$b = 3.920$ (1) Å
$c = 11.738$ (5) Å
$\beta = 111.913$ (5)°
$V = 917.3$ (5) Å^3
$Z = 4$
$D_x = 3.882$ (2) Mg m^{-3}

Synchrotron radiation
$\lambda = 0.872$ Å
Cell parameters from 1332 reflections
$\theta = 5.0$–100.7°
$\mu = 10.34$ mm^{-1}
$T = 95$ K
Shard, black
0.05 × 0.02 × 0.01 mm

Data collection

Bruker SMART APEX diffractometer fitted with an Oxford Cryosystems 600 Series Cryostream Cooler
ω scans
Absorption correction: empirical (*SADABS*; Bruker, 2003)
6862 measured reflections

2500 independent reflections
2499 reflections with $I > -15\sigma(I)$
$R_{int} = 0.043$
$\theta_{max} = 50.5°$
$h = -37 \rightarrow 26$
$k = -4 \rightarrow 6$
$l = -16 \rightarrow 20$

Refinement

Refinement on F^2
$R(F) = 0.076$
$wR(F^2) = 0.069$
$S = 2.15$
2499 reflections

102 parameters
$w = 1/\sigma^2(I)$
$(\Delta/\sigma)_{max} = 0.009$
$\Delta\rho_{max} = 3.17$ e Å^{-3}
$\Delta\rho_{min} = -3.31$ e Å^{-3}

Data were collected with the detector set first at $2\theta = 28°$ and then at $2\theta = 72°$, thus covering reflections up to *ca* $2\theta = 100°$. To optimize the benefits of the higher intensity of a synchrotron beam, a special data collection strategy was used. A complete data set was first collected using the maximum beam intensity, where the detector was saturated for a number of the strong reflections; a second data set was therefore collected with the beam attenuated to such an extent that the strongest low-angle reflection did not saturate the detector. A new data collection was then performed with the detector at $2\theta = 28°$. The occupancy of atom Li3 [0.12 (2)] was refined after setting the U_{iso}(Li3) value equal to U_{iso}(Li1). This is a reasonable constraint since the coordination geometries of atoms Li1 and Li3 are very similar. Atom Li2 was first refined as two partially occupied sites, above and below the inversion centre, in accordance with the model used by Bergström *et al.* (1998). However, as this procedure did not improve the refinement, atom Li2 was finally refined as a single fully occupied site located on the inversion centre. Atoms Li1 and Li3 were both refined with isotropic displacement parameters. After the final refinement cycle, large electron-density residuals were found close to the V2 site.

Data collection: *SMART* (Bruker, 2003); cell refinement: *SAINT+* (Bruker, 2003); data reduction: *SAINT+*; program(s) used to refine structure: *JANA*2000 (Petricek & Dusek, 2000); molecular graphics: *DIAMOND* (Bergerhoff, 1996); software used to prepare material for publication: *JANA*2000.

This work was supported by the Swedish Science Council (VR) and the Swedish Energy Agency (STEM). The authors also thank Y. Cerenius for his technical assistance during the measurements at I711.

Supplementary data for this paper are available from the IUCr electronic archives (Reference: BC1040). Services for accessing these data are described at the back of the journal.

References

Aebi, F. von (1948). *Helv. Chim. Acta*, **31**, 8–21.

Bergerhoff, G. (1996). *DIAMOND*. Version 2.1c. Gerhard-Domagk-Straße 1, Bonn, Germany.

Bergström, Ö., Gustafsson, T. & Thomas, J. O. (1997). *Acta Cryst.* C**53**, 528–530.

Bergström, Ö., Gustafsson, T. & Thomas, J. O. (1998). *Acta Cryst.* C**54**, 1204–1206.

Björk, H., Lidin, S., Gustafsson, T. & Thomas, J. O. (2001). *Acta Cryst.* B**57**, 759–765.

Bruker (2003). *SMART* (Version 5.611) and *SAINT+* (Version 6.45). Bruker AXS Inc., Madison, Wisconsin, USA.

Cerenius, Y., Ståhl, K., Svensson, L. A., Ursby, T., Oskarsson, Å., Albertsson, J. & Liljas, A. (2000). *J. Synchrotron Rad.* **7**, 203–208.

Gustafsson, T., Thomas, J. O., Koksbang, R. & Farrington, G. C. (1992). *Electrochim. Acta*, **37**, 1639–1643.

Höwing, J., Gustafsson, T. & Thomas, J. O. (2003). *Acta Cryst.* B**59**, 747–752.

Höwing, J., Gustafsson, T. & Thomas, J. O. (2004). *Acta Cryst.* B**60**. Submitted.

Kachi, S., Takada, T. & Kosuge, K. (1963). *J. Phys. Soc. Jpn*, **18**, 1839–1840.

Lampe-Önnerud, C. & Thomas, J. O. (1995). *Eur. J. Solid State Inorg. Chem.* **32**, 293–302.

Petricek, V. & Dusek, M. (2000). *JANA*2000. Institute of Physics, Prague, Czech Republic.

Saeki, M., Kimizuka, N., Ishii, M., Kawada, I., Nakano, M., Ichinose, A. & Nakahira, M. (1973). *J. Cryst. Growth*, **18**, 101–102.

Wilhelmi, K. A., Waltersson, K. & Kihlborg, L. (1971). *Acta Chem. Scand.* **25**, 2675–2687.